EFFECT OF LOW-VELOCITY IMPACT DAMAGE ON THE ELECTROMAGNETIC INTERFERENCE SHIELDING EFFECTIVENESS OF CFRP COMPOSITES

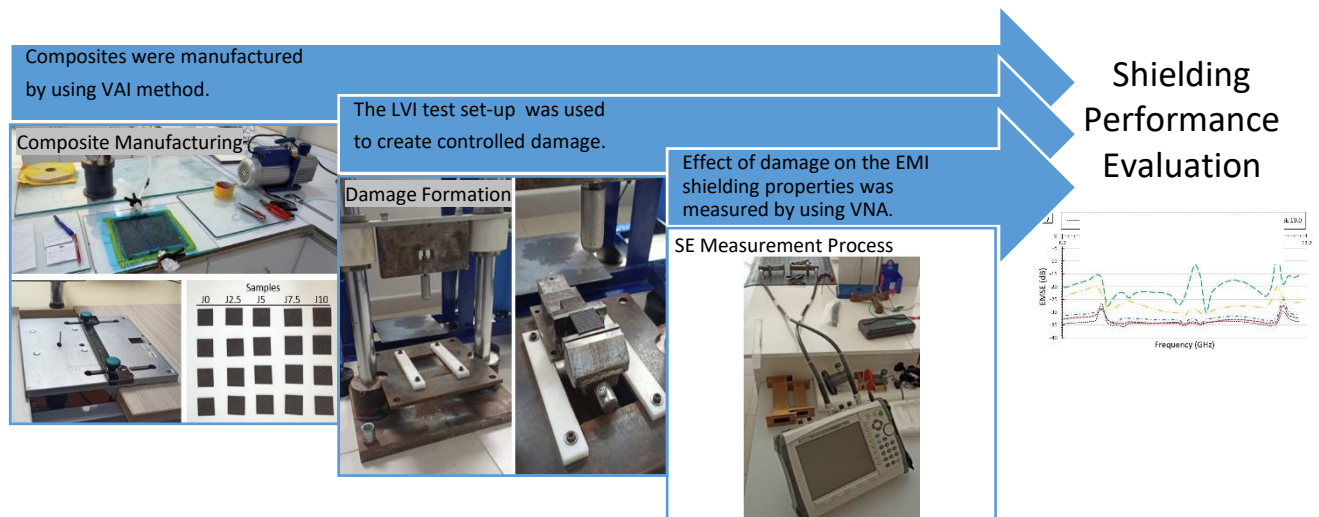***Ferhat YILDIRIM** (ID)

Çanakkale Onsekiz Mart University, Biga Vocational School, Machine and Metal Technologies Department, Çanakkale, TÜRKİYE
ferhatyildirim@comu.edu.tr

Highlights

- Carbon fiber composites are used as EMI shields due to their in plane electrical conductivity.
- However, damages during in use may harm the composite and knowing the EMI performance losses in a strategic product is an important issue.
- Accordingly, the applied 10 joule impact energy to the manufactured composite reduces the electrical conductivity by 74.3% and the EMSE by 40.5%.
- The effect of impact causes fragmentation of matrix and fibers and resulting disconnections of the conductive network of composite.
- 5 joule impact energy is assumed as a threshold value for the composite, and higher impact energies may cause to performance losses that can finish the service life of the 6 layered CFRP composite.
- The deterioration in the carbon-based conductive network, transforms the shielding characteristic from absorbance to reflectance.

Graphical Abstract

Flowchart of the designed experimental study.

*Corresponding Author: Ferhat YILDIRIM, ferhatyildirim@comu.edu.tr

EFFECT OF LOW-VELOCITY IMPACT DAMAGE ON THE ELECTROMAGNETIC INTERFERENCE SHIELDING EFFECTIVENESS OF CFRP COMPOSITES

Ferhat YILDIRIM [iD]

Çanakkale Onsekiz Mart University, Biga Vocational School, Machine and Metal Technologies Department, Çanakkale, TÜRKİYE
ferhatyildirim@comu.edu.tr

ABSTRACT: Carbon fiber reinforced polymer (CFRP) composites are widely used engineering materials in aerospace technologies. These electrically conductive carbon-based materials, due to the lightness advantages, are preferred as shields against electromagnetic radiation, especially in aircraft and satellites. However, the performance losses caused by damage because of flying object collision such as bird, hail, or projectile contain significant uncertainty. Herein, the CFRP composite material was structurally damaged by low velocity impact test set-up at various energy levels between 2.5 to 10 joules, and then its electromagnetic interference (EMI) shielding performance was investigated. In addition, the electrical properties of the material were also examined, and the occurred damage status was evaluated by microscopy studies. Intrinsically, the increase in impact energy increases the grade of damage on body of the material. This results in a drastic decrease in electrical conductivity and EMI performance. In experiments, where 5 joule energy is detected as a threshold level, it has been observed that irreparable damage occurs at energy levels above this value.

Keywords: CFRP composite, Damage, Electromagnetic interference shielding, Electrical conductivity, Low velocity impact

1. INTRODUCTION

The increase in the number of communication devices and electronic systems such as 5G network and GPS satellite signals in recent years has caused increasing electromagnetic (EM) radiations and consequently electromagnetic interference (EMI) [1]. It has been proven by scientific studies that this electromagnetic radiation has many negative effects such as, distortion of wireless phones, radio or TV signals for electronic devices and damaging the DNA and cell structure for living organisms [2, 3]. For this reason, protecting from electromagnetic waves or reducing their effects has become an important research issue [4]. Also, in areas such as military aviation, avoiding EM waves is already an important requirement for strategical aircrafts or satellite. Electromagnetic shielding is known as stopping or limiting electromagnetic radiation with conductive or magnetic barriers and it depends on charge, current and polarization capability of the outer and inner structure of materials [5-7]. Electrically conductive materials come to the forward in this respect, since the shielding is provided by mechanisms such as reflecting the radiation from the outer surface or absorbing it in the inner structure [8]. Metal materials offer good shielding performance due to their electrical conductivity. However, the fact that the main shielding mechanism is reflection, causes the continuation of the damage of the EM effect in different areas with secondary reflections. In addition, the corrosion tendency and high density of metals limiting their usage areas for some sectors such as aviation [9].

Nowadays carbon-based polymer composites are rapidly progressing to become an alternative to metals in terms of EM shielding, as in many other fields [10, 11]. They are preferred for necessary shielding activities, especially in areas such as aviation where low weight is very important. Moreover, easy processibility and the structural diversity of carbon (particle, fiber, foam, etc.) offers a wide range of usage options in different fields [12]. Long service life and low maintenance requirements are other important factors for the use of composite materials as shielding elements [13, 14]. However, deformations and

---

*Corresponding Author: Ferhat YILDIRIM, ferhatyildirim@comu.edu.tr

possible damages due to usage conditions can occurs. According to the report of European Aviation Safety Agency [15], the kinetic energy at the time of collision of an aircraft and a bird (bird masses above 0.78 kg) can reach up to 1500 joule. According to the same report, it was stated that this value is 2.7 to 6.6 times higher than the minimum requirements for fixed wing aircraft with certification requirements. It is emphasized here that speed and mass are the main factors determining the energy and constitute new areas on material performances that need to be examined. These impacts can result in mechanical electrical or EMI performance losses in composites as in every material. For example, a stealth capable aircraft or drone may be damaged while on duty, such as hail, projectile or bird strikes, and any deformations like scratching, cracking, or bending may occur on the structural shield material [16]. So, the electromagnetic wave will leak from the damaged area of the body and effect all system performance. This may cause it to lose the invisibility advantage that it gained by absorbing radar waves. It is vital that military vehicles and devices do not lose their EMI performance to maintaining their combat survivability [17]. This makes it necessary to constantly monitor the performance losses of materials due to damage against similar cases.

Some studies in the literature reveal that changes occur in electrical and shielding properties even under limited deformation conditions to which materials are exposed. For example, some researchers studying flexible film and foam materials have reported the electrical conductivity and EMI performance of the material decreasing when bending application. Yang et al. found that the average EMI performance decrease from 26.5 dB to 25.8 dB and resistivity slightly increase after continuous bending (1000 cycles) process on their study that investigate the flexible silicon rubber/CNT/Fe3O4 nanocomposite characterization [18]. Similarly, Jiang et al. investigated the thermoplastic polyurethane/reduced graphene oxide composite materials. They found that the thin foam materials EMI values decreased from 21.5 dB to 16.5 dB at 1000 cycled and 2 mm curvature radius bending period [19]. Ravindren et al. have tested the ethylene-co-methyl acrylate (EMA), ethylene octene copolymer (EOC), and carbon nanotube (CNT) composites in terms of EMI properties. They found that the average EMI decrease from 33 dB to 32 dB after 500 cycled bending process [20]. Zhou et al. investigated the electrical conductivity of the graphene/carbon nanotube hybrid composite films after multiple bending movement. They pointed out the electrical conductivity slightly decrease after 1000 cycled bending at smaller than 1 mm curvature radius [21].

Wei et al. studied the effect of CNT coating on electrical conductivity properties of pre-cracked and rolled GFRP composites samples. The results showed that CNTs help maintain electrical conductivity while cracks develop, the conductivity decrease while the mechanical strain occurred by rolling [22]. Some studies have focused on self-healing mechanisms to compensate for the loss of performance caused by damage. Sim et al. studied on self-healing graphene oxide/silver nanowire films and textile. They found that the EMI SE was decreased from 72 dB to 56 dB, the resistivity was increased from 15 to 40 MΩ when the samples were cracking damaged. They also declared that the self-healed material regains the similar EMI performance again with 71 dB [13]. Ma et al. were able to develop a MXene melamine sponge mechanism that regain performance at ratio of 99.99% after breaking damage by repairing itself with the application of PU substrate [23]. Wang et al. researched the CNT reinforced dynamic crosslinked polyurethane (PUDA) polymer composite as a self-heal material. They declared when the sample cracked the EMI value decrease from 30.7 dB to 16.8 dB. Also, their self-healing mechanism repaired itself approximately at ratio level of 97% after multiple cracking-healing cycles [24] On another study of Wang et al. they found that the EMI value decrease from 35.5 dB to 17.1 dB after cracked by blade and EMI value decrease from 33.8 dB to 32.3 dB after 5000 times bending at another CNT reinforcement level [16].

There are different studies too, showing that the need for EMI shielding is not just aviation oriented. The same performance can be expected from buildings that will protect ground personnel from bursts of electromagnetic radiation. Yoo et al. investigated the CNT added cement that proposed for construction of military building designed against to protect electromagnetic radiation. They pointed out CNT reinforcement offers beneficial EMI performance in the construction but emphasized that the EMI performance decrease when the microcracks occurred on the cement [25]. Kim et al reported similar results on CNT reinforced concrete. They said that the EMI performance decreases approximately levels of 40-

50% compared to the non-cracked samples when different sized cracks that detected with image processing and appear on samples [26].

The main subject of all these studies presented in the literature is depending on the operational conditions, many cracks or damage may occur in the composites and the material may not give expected performance. For this reason, the relationship between damage in the structure and EMI shielding effectiveness should be evaluated. Most of the literature focuses on the electrical and EMI performance loss and healing properties of flexible, film, and foam materials. Unlike the literature, the study focuses on the damage-loss relationship of the most basic composite material currently in use on aviation sector such as aircraft bodies, landing gear covers, satellite housing elements, electronic device boxes etc. However, post-damage EMI performances of CFRP composites, which are widely used in areas such as military aviation, have not been extensively investigated. In this study, changes in electrical conductivity and electromagnetic shielding performance of CFRP composites that damaged by various level of impact energies were investigated experimentally. Thus, an analysis on damage resulted shielding performance losses that may occur during service life, especially aircraft or drones, has been tried to be presented.

2. MATERIAL AND METHODS

2.1. Materials

Used carbon fiber fabric as the reinforcement material in the study has 7 µm diameter and 240 gr/m² density with twill woven. The epoxy matrix with two components as known commercial code MGS L285/H285 has aviation certificated and both materials was purchased from Dost Kimya, Türkiye.

2.2. Manufacturing of Samples

The vacuum infusion method was chosen for the composites manufacturing (Figure 1). Thus, it was aimed to produce samples with the balanced matrix distribution and stable thickness. The carbon fabrics prepared by cutting in size of 300×300 mm was arranged in 6-layers and after the peel ply and vacuum net were added, the layers were covered with vacuum nylon. After resin infused the composite was cured at room temperature for 8 hour and post cured at 70 °C in an oven for 2 hours. 20 samples were prepared by cutting the composite in 40×40 mm that manufactured according to the designed experimental setup.
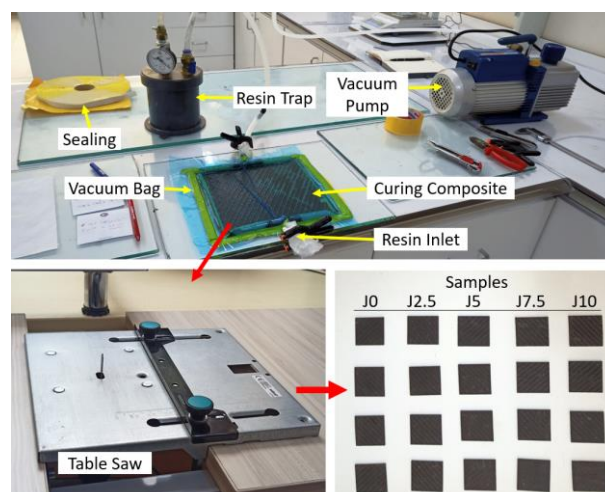
Figure 1. Composite manufacturing and sample preparation.

Although it is common application to positioned Teflon or nylon film between fabric layers for obtaining crack in the literature, these samples are used in Mode-I and Mode-II interlaminar shear tests [27]. In addition, since these cracks occur between the layers and in plane direction, they are incompatible

with the subject of this study and therefore they were not preferred. On the other side, scratching with a knife is another way to obtaining crack [24]. But this application preferred for sponge, film or foam materials and because of the regularity shape does not coincide with natural damage case. Thus, the low velocity impact test device given in Figure 2 was used to create damage on the samples.
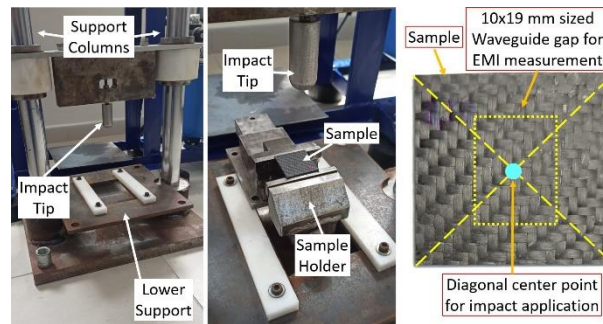

Figure 2. Impact application set-up.

Since the aim of this study is mapping the EMI shielding performance loss, 2.5, 5, 7.5, and 10 joule impact energy values were chosen as the main examination range. A possible hail, bird or any other particle strike scenario was tried to be obtained by applying four different energy level of impact to the 40×40 mm samples that positioned on the sample holder. The impact was applied to the diagonal center of the samples. For this aim steel impact tip that has 10 kg mass were dropped from a height of 25, 50, 75, and 100 mm, respectively. The used potential energy formula has been given in equation 1. Accordingly, 4 samples were used for impact application at each energy level, and 3 measurements were made for EMI and 7 measurements were made for electrical conductivity on each sample after damage occurred. Experimental design has been given in Table 1.

$E=mgh$ (1)

Here are the E is energy (joule), m is the mass (kg), g is gravity (m/s^2 and it is assumed as 10), and h is the height (m).

Table 1. Experimental parameters and sample codes.

Sample Code	Applied Impact Energy (J)	Impact height (mm)	Impact speed (m/s)
J0	0	0	0
J2.5	2.5	25	0.707
J5	5.0	50	1
J7.5	7.5	75	1.224
J10	10.0	100	1.414

2.3. Experimental procedure

Electrical conductivity has a direct effect on EMI. In order to examine the EMI performance of the material, it is necessary to measure the electrical conductivity of the material. Only in this way damage and EMI can be linked each other established and discussed. Two probe method was used for measuring electrical conductivity of composite materials with using an ohmmeter according to ASTM D4496-13. The electrical resistance and resistivity were calculated using following equations from 2 to 4 [28].

$R=V/I$ (2)

$\rho=(R\times A)/l$ (3)

$\sigma=1/\rho$ (4)

Here are the ρ is resistivity, R is resistance (ohm), and V is electric potential difference (Voltage). Cross-sectional of measured area is A (cm²), contact length of probes l (cm), and electrical conductivity is σ (S/cm).

The vector network analyzer with two WR-90 waveguide set was used for electromagnetic shielding effectiveness (EMSE) measurements at X-band (8.2–12.4 GHz). Electromagnetic frequency, consisting of 8.2 and 12.4 GHz frequencies, is referred to as X-Band. It is widely used in many sectors, especially in aviation, defiance, marine and satellite systems, for radar observation, navigation, communication and meteorological forecasting [29]. These properties of the X-Band have enabled to selected as the target frequency range of the study especially focused aviation materials. On the other hand, the used waveguide technique is one of the non-standardized SE measurement techniques according to the IEEE 2715-2023 standard report document. it is a combination of ASTM D-4935 and IEEE-299 standards. It has a very popular and widespread usage areas thanks to its easy application, small sample size requirement and ability to measure high frequencies such as 8.2-12.4 GHz [9, 27, 29-34]. In this technique, the samples were positioned between two insulating sample holder that they have 10×19 mm sized gap by aligning the center of the impact and waveguide gap. Thus, it was ensured that the samples were not fragmented due to cracks and that the scattering S parameters were measured only with electromagnetic waves that spreading from the waveguide and crossing passed through the gap of sample holder [35, 36].

Total shielding effectiveness (SE$_{Tot}$) was calculated using following equation 5. SE$_{Tot}$ is equal to sum of shielding effectiveness of reflectance (SE$_R$), shielding effectiveness of absorbance (SE$_A$), and shielding effectiveness of multiple inner reflectance (SE$_M$). SE$_M$ is neglected, when the SE$_{Tot}$ is greater than ±10 dB [9].

$$SE_{Tot}\ (dB) = SE_R + SE_A + SE_M = 10\log(\frac{P_t}{P_i}) \tag{5}$$

Here are, the power of the incident electromagnetic waves is P_i and power of transmitted electromagnetic waves is P_t. The required SE_A, SE_R, and SE_T parameters were calculated by using the following equations from 6 to 8 according to the measured S parameters with network analyzer [36, 37].

$$SE_A(dB) = 10\log(\frac{1-S_{11}{}^2}{S_{12}{}^2}) = 10\log(\frac{1-S_{22}{}^2}{S_{21}{}^2}) = 10\log(\frac{1-R}{T}) \tag{6}$$

$$SE_R(dB) = 10\log(\frac{1}{1-S_{11}{}^2}) = 10\log(\frac{1}{1-S_{22}{}^2}) = 10\log(\frac{1}{1-R}) \tag{7}$$

$$SE_T(dB) = 10\log(\frac{1}{S_{12}{}^2}) = 10\log(\frac{1}{S_{21}{}^2}) = 10\log(\frac{1}{T}) \tag{8}$$

Here are, the absorbance is A, the reflectance is R and the transmittance is T. To verification of the system, the sum of A, R and T must be equal to 1 [36, 37].

The penetration ability of electromagnetic radiations into an electrically conductive material is limited to its surface thickness that related with charge current and polarization, also known as the skin effect. The shielding effectiveness of absorption is inversely proportional to the skin depth (δ), where the field reduces to 1/e of the incident value [38, 39]. The relation between SEA and skin depth is calculated by using equation 9 [40].

$$\delta = -8.68\left[\frac{t}{SE_A}\right] \tag{9}$$

Finally, the SOIF BK5000 optical microscope (OM) was used to investigate the microstructure and crack propagation of composites due to the impact application.

3. RESULTS AND DISCUSSIONS

3.1. Electrical properties

The electrical conductivity and resistivity tests results are given in Figure 3. The damaged materials offer various resistivity and conductivity values according to applied impact energy levels. The measurements show that the electrical resistance increases as the damage on the material increases. While the non-damaged J0 sample gave a resistivity value of 25.64 Ωcm, the resistivity of the most damaged J10 sample increased approximately 3.7 times and was calculated as 95.84 Ωcm. Similarly, the intrinsic conductivity values change inversely with the damage. While the intrinsic conductivity value for the undamaged J0 sample was 0.039 S/cm, it was calculated as 0.01 S/cm for the damaged J10 sample. The effect of the damage on the electrical conductivity values can be analyzed better in the drawn graph.
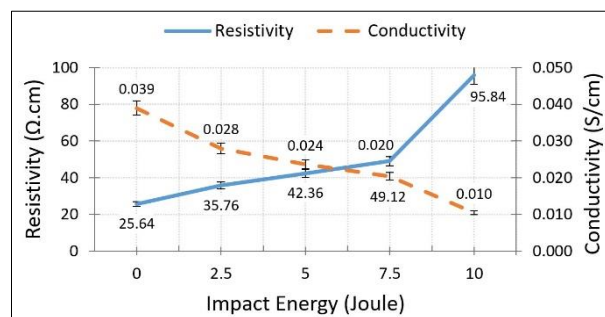
Figure 3. Electrical conductivity and resistivity results.

The literature reveal that changes occur in electrical properties under limited deformation conditions to which materials are exposed [18-21]. Wei et al. declared that the electrical conductivity decreases while the mechanical strain occurred and cracks develop on GFRP composites [22]. It is thought that the main reason of this change in conductivity and resistivity is the fragmentation of carbon fibers by impact. The integrity of the fragmented and separated carbon fibers is disrupted, and this reveals that the existing electrical network is weakens and broken. In other words, the reduced ability of electron transfer leads to an increase in the resistance of the material, resulting in a decrease in its conductivity [41, 42]. It is observed that the J10 sample, damaged with 10 joule impact energy, shows a large jump in resistivity results. This change in electrical properties also gives us information about the damage status of the material and suggests that the larger area of damage occurred in this sample. Because the increase in resistance for equivalent material and fixed probe range is explained by the reduction of the cross-sectional area according to the formulation [28]. Here, change in contact area of fibers can be calculated by operating the formula in reversely in accordance with resistivity-area relationship of the J0 sample and the resistance values of the J2.5, J5, J7.5, and J10 samples. Accordingly, observed decrease in contact area proves the existence of broken and fragmented fiber groups [25, 26]. It should be noted that although the formula defines a 2-dimensional area, it is possible the fracture can be occurred in 3-dimensional formation. Because the weaving of carbon fiber fabric is 0-90 twill knitted. Warp and weft weaving makes it possible to crack propagate in both the X and Y directions. However, when the effect of the impact force in the Z direction is added to material, the vectoral forces promote the fracture formation in all 3-dimensions. Accordingly, as the impact energy increases, the damage on the material is spreading, and the contact area of the fibers decreases due to fiber fragmentation. Finally, decrease on area of carbon fibers that contact with each other, it results in a decrease in electrical conductivity [25, 26]. The relationship between the impact energy and the contact area of fibers are given in Figure 4.
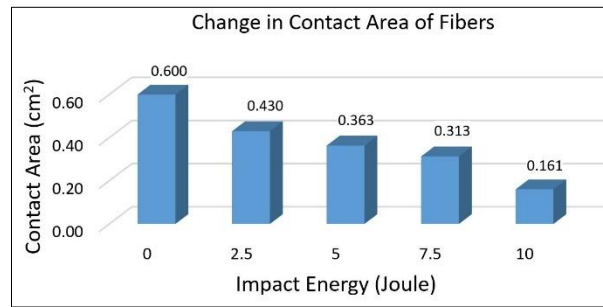
Figure 4. Relationship between the impact energy and the contact area of fibers according to the resistivity measurements.

3.2. Shielding Effectiveness (SE) results

The SE Tot results as a function of the frequency are presented in Figure 5a. Non-damaged J0 sample gives -33.928 dB SE Tot value. The calculated SE Tot values of other samples J2.5, J5, J7.5, and J10 are -33.175, -31.956, -26.745, and -20.184 dB, respectively. The drastic decrease on SE Tot can easily see when the impact energy increase. Decrease rates for J2.5, J5, J7.5, and J10 were calculated as 2.2, 5.8, 21.1, and 40.5% compared to the J0, respectively. Electrical conductivity plays an important role in attenuating EM waves on the material [9, 41, 43]. As EM waves move through the structure, they dispersed by electrical charge transportation and is absorbed by converting to heat [4, 44, 45]. Therefore, the width of the conductive mesh is important. Since the epoxy matrix is an insulator, it is completely permeable to EM waves. In other words, epoxy has no efficient shielding ability [29]. The occurred damage by the impact does not change this effect, too. So, it can be said that the epoxy matrix is not responsible for decrease of shielding ability. The damage, caused by the impact means the breaking and fragmentation of the carbon fibers as much as the matrix fragmentation. Thus, electrically conductive networks get weakens and the impedance mismatching between material surface and air is reduces [8, 20, 41, 46]. The SE Tot values decreased with the reduce of electrical conductivity due to the damage occur. Thus, non-damaged J0 sample gives the highest SE Tot due to all fibers stay together, contrary the J10 has the minimum SE Tot value.

Although the first noticeable result is the dramatic decrease in SE Tot values another interesting issue is the stability of the respond to EM waves is impaired and the frequency range at which it exhibits sensitivity is expanding. As can be seen from the reduction of the straight sectors of the curve the sensitivity range shown at the frequencies of 8.8 and 11.8 GHz has expanded to 8.5-9.0, 9.8-10.5, and 11.4-12.0 GHz ranges. This proves the serious SE Tot performance losses occurs in the material. Also, while the J0 sample easily reaches up the commercially required -30 dB SE Tot values [4, 47, 48], only the J2.5 and J5 samples have been able to maintain its effectiveness. The other J7.5 and J10 samples shows enormous performance decrease after impact damaged. Thus, it is obviously seen that shield could not fulfill her duty and the materials should be fix or replaced with a backup before any other usage.
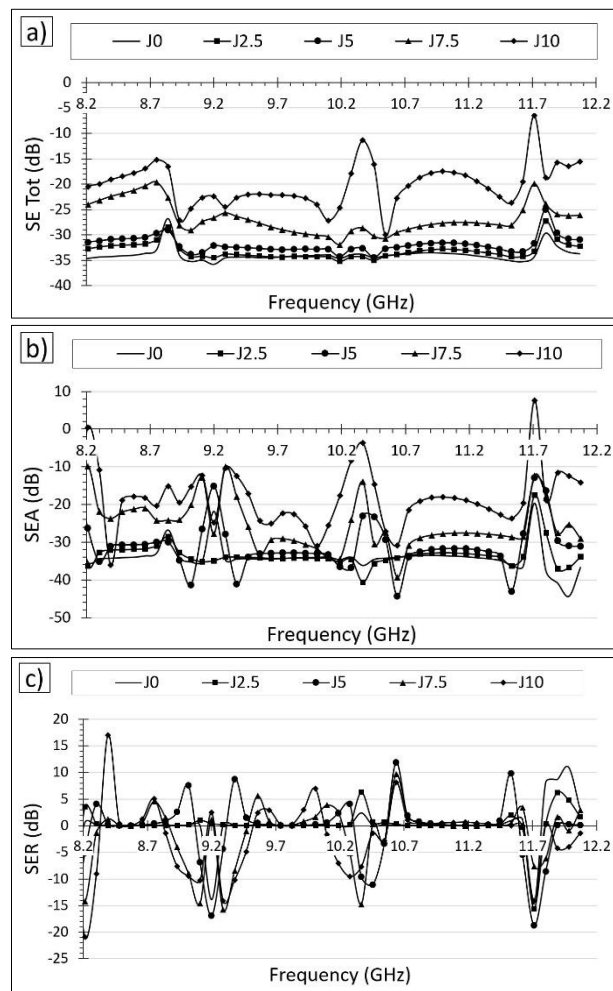
Figure 5. Shielding results of the damaged samples; a) SE Tot, b) SEA, and c) SER.

Figure 5b and 5c gives the SEA and SER results of the samples. The trend of SEA curves show similarity with the EMSE curves. While absorbance lines are clustered around -33 dB and shifted towards the zero as the impact energy increased, reflectance lines are located on the center zero region. Another information that can be obtained from the curves is that the absorption sensitivity of the material is impaired. According to the literature, materials that provide excellent shielding performance offers flatter curves [13, 23]. The fact that the curves of the damaged samples has more zigzag shape indicates that the reduces ability of response according to the changing frequency. Although the mean values seem numerically significant, the shielding change observed at close frequencies reveals that the characteristic of the material is deteriorated.

Figure 6 gives the comparison of SE Tot, SEA, and SER results. The SEA values of the samples J0, J2.5, J5, J7.5, and J10 are calculated as -33.868, -33.077, -30.857, -25.316, and -18.310 dB, respectively. The SER values was also calculated as -0.061, -0.098, -1.098, -1.429, and -1.873 dB for J0, J2.5, J5, J7.5, and J10 samples, respectively. The obtained results reveal that the main shielding mechanism of the composite material is absorbance. The absorption dominated shielding characteristic is, proving its potential for use in applications where low radar visibility and high electronic protection is required [49].
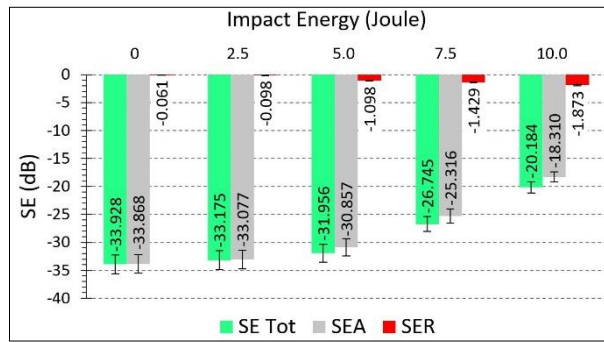
Figure 6. Comparison of SE Tot, SEA, and SER results.

However, the absorbance ability of the material decreases significantly with the damage caused by the impact. As in the SE Tot, decrease from -33 dB to -18 dB show an absorption performance loss at ratio of 45%. The results reveal that the conductive network which the electromagnetic wave propagates in the material is damaged. In fact, this situation shows parallelism with the decreasing in electrical conductivity. In addition, while the absorbance decreases, the EM reflectance values of the material significantly increase. The calculated increase rate is about 2970%. It is thought that the increased micro surface area due to the fractured fibers lead to more reflection of EM waves. It has been stated in the literature that surface-enlarging factors such as intra-structure pores increase the reflection [38]. The findings can be considered as a comment compatible with the literature. This marginal increase means that the shield lost its mission capability by turning EM waves into the reflection after a damage due to the impact while absorbing radar waves.

The skin depth, which is the effective thickness that EM waves is absorbed by dispersing in the material and related with frequency, material permeability, and conductivity [39, 50]. The calculated skin depth values for all materials are given in the Figure 7. The calculated skin depth of the non-damaged J0 sample is 0.512 mm versus 33.868 dB SEA value. This value is the required thickness for absorbing EM waves of CFRP composite material during shielding. Carbon fibers increase impedance mismatching and skin depth with lower magnetism and high electrical conductivity [38]. The other skin depths were calculated as 0.524, 0.532, 0.685, and 0.948 for J2.5, J5, J7.5, and J10 samples, respectively. As can be seen on combine graph at Figure 7, while the applied impact energy increases, the thickness required by the material for absorbance increases due to the conductive network damaged that emits EM waves. Even though the absorbance value offered by the material decreased from -33 dB to -18 dB, the skin depth value increased almost 2 times from 0.512 mm to 0.948 mm. These values show the size of the damage on the J10 sample and how effects the material shielding characteristics. In another aspect, the calculated skin depth differences quite little between the J0, J2.5, and J5 samples, which reveal that the damage is formed at a small area (occurred on material surface) for J2.5 and J5 samples. Therefore, it can be said that there was no internal structure damage has occurred for these materials at the impact energies mentioned. In addition, this result is confirmed in the "microscopy studies" section by images that obtaining from optical microscope.
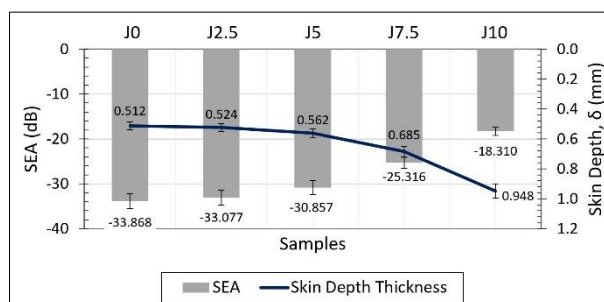

**Figure 7.** Skin depth absorbance relation versus impact energy.

3.3.   Optic microscopy studies

Optical imaging studies are important in terms of investigating the causes of the change observed in electrical and shielding properties. The impact zone images given in Figure 8 prove the fiber fragmentation hypothesis. With the increasing impact energy, the damage area grows and deepens. Although the absolute area cannot be calculated exactly, it was detected that the damage size increased exponentially while the impact energy increased linearly. In addition, while the damage was observed only on the surface for J2.5 and J5 samples, it was developed in penetration and form of complete disintegration for J7.5 and J10 samples. In other words, while the damage is 2D (X-Y plane) for J2.5 and J5, it is occurred on 3D (X-Y plane and Z direction) for J7.5 and J10. Considering that the repairability and reusability, it is thought that renovation is possible for J2.5 and J5 samples, since the damage occurs on the surface. However, since the damage deeply penetrated into structure and resulted with dividing in two parts, it is thought that it is not possible to repair it efficiently for J7.5 and J10 samples.
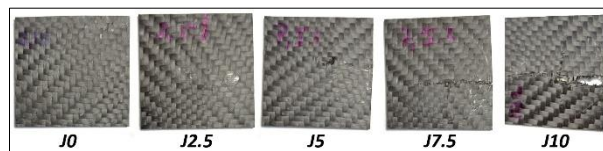
Figure 8. Makro images of samples after impact application.

The damage size, which is relatively low for J2.5 sample, increases rapidly for the J5, J7.5 and J10 samples with the increase of impact energy. While a very deep crack was formed in Z direction for J7.5, the full separation limit was reached for J10 sample. The observed great damage illuminates the reason for the conductivity and therefore SE losses of the materials in line with the literature [22, 25, 26]. Magnified images of the damage areas are presented in Figure 9. It can be seen in Figure 9a, that the damage in J2.5 in the form of matrix fracture and is superficial. It was observed that some of the fibers in the top layer of composite were broken for a very limited area and the damage did not progress into the structure. As given in Figure 9b, it was determined that the matrix cracked more intensely in the J5 sample, and the top carbon fiber bundle completely separated from each other at woven intersection region in the plane direction. Some cracks have been measured average width of 100 μm. As can be seen in Figure 9c, there is a significant damage on the J7.5 sample. The average crack widths are around 300 μm and they penetrate deeply into the composite. Unlike the J5 samples, the damage occurred suddenly and in the form of complete breakage without waiting for the cracks reach up to the warp-weft intersection regions. As given in Figure 9d, J10 samples were completely fragmented. The material was not only separated in the plane direction but also delaminated due to the impact. Multiple damage occurred at various direction and delamination between the layers have increased the loss of conductivity. And thus, shielding performance against to EM waves decreased to levels that render the product useless.
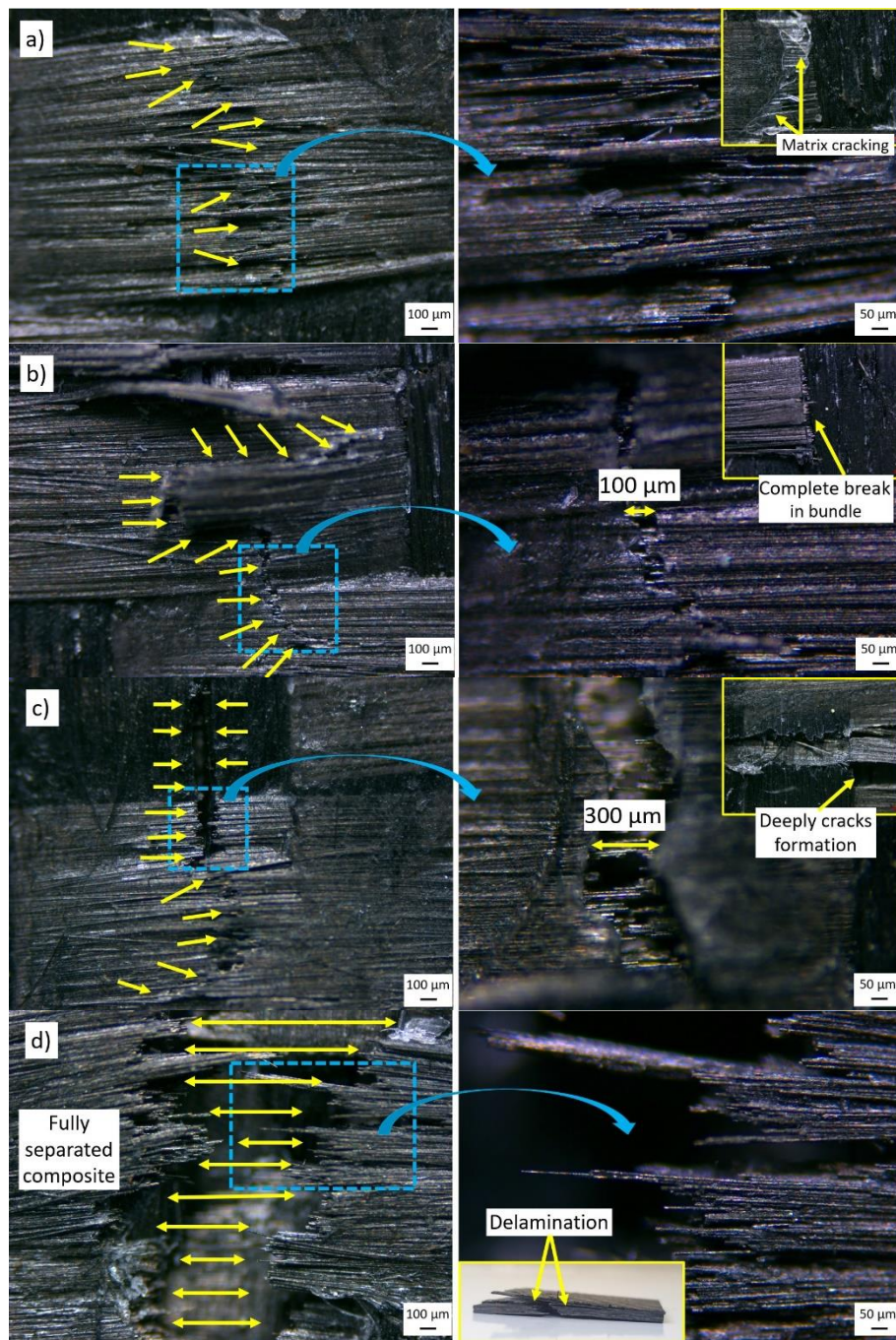
Figure 9. OM images of the samples, a) J2.5, b) J5, c) J7.5, and d) J10.

In terms of the repairability of the material, it is considered that repair is possible in the J2.5 and J5 samples, since the damage occurred on the surface. In addition, even though these two samples suffer 2.2% and 5.8% performance loss in EM shielding, they are still above the 30 dB commercially required shielding limit. However, since the damage in J7.5 and J10 samples is affecting the internal structure of the material, it is thought that it is not possible to repair it. Thus, it can be concluded that the impact energy of 5 joule is the threshold value for a composite material designed as in the study. It is considered that the material exposed to values above 5 joules, it can no longer in use due to the damage.

4. CONCLUSIONS

This study addresses the effect of the damages after low velocity impact at various energy levels (2.5, 5, 7.5, and 10 joules) on the electrically conductivity and the EMSE performance of carbon fiber reinforced polymer composite. According to the results, the electrical resistance increases as the damage on the material increases. While the non-damaged J0 sample gave a resistivity value of 25.64 Ωcm, the resistivity of the most damaged J10 sample increased approximately 3.7 times and was calculated as 95.84 Ωcm. One of the other findings of the study is that the 6-layer CFRP composite can easily reach up the 30 dB SE Tot level that require for commercial products. While non-damaged J0 sample gives -33.928 dB SE Tot value, the other samples J2.5, J5, J7.5, and J10 are -33.175, -31.956, -26.745, and -20.184 dB, respectively. The applied impact energy has a direct effect on the damage that occurred on the material. The damage that grows with increasing impact energy, weakens the electrically conductive network on the material. Since SE is associated with electrical conductivity, decreasing conductivity reduces the shielding performance of the material. Decrease rates for J2.5, J5, J7.5, and J10 were calculated as 2.2, 5.8, 21.1, and 40.5% compared to the J0, respectively. This proves the hypothesis, that impact damages can reduces the SE performance of CFRP composites. The SEA values of the samples J0, J2.5, J5, J7.5, and J10 are calculated as -33.868, -33.077, -30.857, -25.316, and -18.310 dB, respectively. The results prove that main shielding mechanism of the produced composite is absorbance. However, the absorbance ability of the material decreases significantly with the damage caused by the impact. As in the SE Tot, decrease from -33 dB to -18 dB show an absorption performance loss at ratio of 45%. 5J impact energy is a threshold value for the material, and greater impact energies may cause to shielding performance losses that can finish the service life of the material. In addition, the deterioration in the carbon-based conductive network with the impact damage, transforms the shielding characteristic of the material from absorbance to reflectance. Finally, microscopy studies have shown that it is difficult to repair the damaged material due to the completely broken, for gaining shielding capability again. Accordingly, it can be recommended that the materials should be designed considering the effects of the harsh conditions they may encounter during their duties and that they should be constantly checked.

Declaration of Ethical Standards

The author declares that all ethical guidelines including authorship, citation, data reporting, and publishing original research are followed.

Declaration of Competing Interest

The author declares that there is no conflict of interest.

Funding / Acknowledgements

This study did not receive funding from any provider.

Data Availability

The data that support the findings of this study are available from the corresponding author upon reasonable request.

REFERENCES

[1]   M. Han, C. E. Shuck, R. Rakhmanov, D. Parchment, B. Anasori, C. Min Koo, G. Friedman, and Y. Gogotsi, "Beyond Ti3C2Tx: MXenes for Electromagnetic Interference Shielding", *ACS Nano*, vol. 14, no. 4, pp. 5008–5016, 2020.

[2]   D. Carpenter, "Human disease resulting from exposure to electromagnetic fields", *Reviews on Environmental Health*, vol. 28, no. 4, pp. 159-172, 2013.

[3]   D. A. Yilmaz, İ. H. Çağiran, G. Dege, and M. S. Yildirim, "Effects of Electromagnetic Pollution on Health", *MAUNSagBil.Derg*. vol. 2, no. 2, pp. 67-79.

[4]   D. Munalli, G. Dimitrakis, D. Chronopoulos, S. Greedy, and A. Long, "Electromagnetic shielding effectiveness of carbon fibre reinforced Composites", *Composites Part B*. vol. 173, pp. 106906, 2019.

[5]   D. D. Soyaslan, "Design and Manufacturing of Fabric Reinforced Electromagnetic Shielding Composite Materials", *Textile and Apparel*, vol. 30, no. 2, June, pp. 92-98, 2020.

[6]   X. Jia, Y. Li, B. Shen, and W. Zheng, "Evaluation, fabrication and dynamic performance regulation of green EMI-shielding materials with low reflectivity: A review". *Composites Part B* vol. 233, pp. 109652, 2022.

[7]   H. Abbasi, M. Antunes, and J. I. Velasco, "Recent advances in carbon-based polymer nanocomposites for electromagnetic interference shielding", *Progress in Materials Science*, vol. 103, pp. 319-373.

[8]   Y. Chen, L. Pang, Y. Li, H. Luo, G. Duan, C. Mei, W. Xu, W. Zhou, K. Liu, and S. Jiang, "Ultra-thin and highly flexible cellulose nanofiber/silver nanowire conductive paper for effective electromagnetic interference shielding", Composites Part A, vol. 135. pp. 105960, 2021.

[9]   F. Yıldırım, E. Kabakçı, H. S. Şaş, and V. Eskizeybek, "Multi-walled carbon nanotube grafted 3D spacer multi-scale composites for electromagnetic interference shielding", *Polymer Composite*, vol. 43, pp. 5690, 2020.

[10]   M. S. Cao, W. L. Song, Z. L. Hou, B. Wen, and J. Yuan, "The effects of temperature and frequency on the dielectric properties, electromagnetic interference shielding and microwave-absorption of short carbon fiber/silica composites", *Carbon*, vol. 48, no. 3, pp. 788-796, 2010.

[11]   J. M. Thomassin, C. Jérôme, T. Pardoen, C. Bailly, I. Huynen, and C. Detrembleur, "Polymer/carbonbased composites as electromagnetic interference (EMI) shielding materials", *Materials Science and Engineering: R*, vol. 74, no. 7, pp. 211-232, 2013.

[12]   R. Kumar, S. Sahoo, E. Joanni, R. K. Singh, W. K. Tan, K. K. Kar, and A. Matsuda, "Recent progress on carbon-based composite materials for microwave electromagnetic interference shielding", *Carbon*, vol. 177, pp. 304-331, 2021.

[13]   H. J. Sim, D. W. Lee, H. Kim, Y. Jang, G. M. Spinks, S. Gambhir, D. L. Officer, G. G. Wallace, and S. J. Kim, "Self-healing graphene oxide-based composite for electromagnetic interference shielding", *Carbon*, vol. 155, pp. 499-505, 2019.

[14]   H. Zhang, X. Zheng, R. Jiang, Z. Liu, W. Li, and X. Zhou, "Research progress of functional composite electromagnetic shielding materials", *European Polymer Journal*, vol. 185, pp. 111825, 2023.

[15]   European Aviation Safety Agency, "Bird Strike Damage & Windshield Bird Strike Final Report", 5078609-rep-03 Version 1.1,

[16]   T. Wang, W. C. Yu, W. J. Sun, L. C. Jia, J. F. Gao, J. H. Tang, H. J. Su, D. X. Yan, and Z. M. Li, "Healable polyurethane/carbon nanotube composite with segregated Structure for efficient electromagnetic interference shielding", *Composites Science and Technology*, vol. 200, pp. 108446, 2020.

[17]   W. Cai, N. Shao, X. Shao, and Z. Pan, "Structural analysis of carbon clusters by using a global optimization algorithm with Brenner potential", *Journal of Molecular Structure: THEOCHEM*, vol. 678, no. 1–3, pp. 113-122, 2004.

[18]   J. Yang, X. Liao, J. Li, G. He, Y. Zhang, W. Tang, G. Wang, and G. Li, "Light-weight and flexible silicone rubber/MWCNTs/Fe3O4 nanocomposite foams for efficient electromagnetic interference shielding and microwave absorption", *Composites Science and Technology*, vol. 181, pp. 107670, 2019.

[19]   Q. Jiang, X. Liao, J. Li, J. Chen, G. Wang, J. Yi, Q. Yang, and G. Li, "Flexible thermoplastic polyurethane/reduced graphene oxide composite foams for electromagnetic interference shielding with high absorption characteristic", *Composites Part A: Applied Science and Manufacturing*, vol. 123, pp. 310-319, 2019.

[20] R. Ravindren, S. Mondal, K. Nath, and N. C. Das, "Investigation of electrical conductivity and electromagnetic interference shielding effectiveness of preferentially distributed conductive filler in highly flexible polymer blends nanocomposites", *Composites Part A: Applied Science and Manufacturing*, vol. 118, pp. 75-89, 2019.

[21] E. Zhou, J. Xi, Y. Guo, Y. Liu, Z. Xu, L. Peng, W. Gao, J. Ying, Z. Chen, and C. Gao, "Synergistic effect of graphene and carbon nanotube for high-performance electromagnetic interference shielding films", *Carbon*, vol. 133, pp. 316-322, 2018.

[22] L. Wei, N. Li, G. D. Wang, X. L. Liu, Y. X. Liu, and Y. C. Shen, "The effect of rolling process on the mechanical and electrical properties of CNTs-enhanced GFRP", *Materials Today Communications*, vol. 32, pp. 103998, 2022.

[23] W. Ma, W. Cai, W. Chen, P. Liu, J. Wang, and Z. Liu, "A novel structural design of shielding capsule to prepare high-performance and self-healing MXene-based sponge for ultra-efficient electromagnetic interference shielding", *Chemical Engineering Journal*, vol. 426, pp. 130729, 2021.

[24] T. Wang, W. C. Yu, C. G. Zhou, W. J. Sun, Y. P. Zhang, L. C Jia, J. F Gao, K. Dai, D. X Yan, and Z. M. Li, "Self-healing and flexible carbon nanotube/polyurethane composite for efficient electromagnetic interference shielding", *Composites Part B: Engineering*, vol. 193, pp. 108015, 2020.

[25] D. Y. Yoo, M. C. Kang, H. J. Choi, W. Shin, and S. Kim, "Electromagnetic interference shielding of multi-cracked high-performance fiber-reinforced cement composites – Effects of matrix strength and carbon fiber", *Construction and Building Materials*, vol. 261, pp. 119949, 2020.

[26] S. Kim, Y. S. Jang, T. Oh, S. K. Lee, and D. Y. Yoo, "Effect of crack width on electromagnetic interference shielding effectiveness of high-performance cementitious composites containing steel and carbon fibers", *Journal of Materials Research and Technology*, vol. 20, pp. 359-372, 2022.

[27] G. Mutlu, F. Yıldırım, H. Ulus, and V. Eskizeybek, "Coating graphene nanoplatelets onto carbon fabric with controlled thickness for improved mechanical performance and EMI shielding effectiveness of carbon/epoxy composites", *Engineering Fracture Mechanics*, vol. 284, pp. 109271, 2023.

[28] D. Mi, X Li, Z Zhao, Z Jia, and W. Zhu, "Effect of dispersion and orientation of dispersed phase on mechanical and electrical conductivity", *Polymer Composites*, vol. 42, pp. 4277, 2021.

[29] V. Zaroushani, A. Khavanin, S. B. Mortazavi, and A. J. Jafari, "Efficacy of Net Epoxy Resin for Electromagnetic Shielding in X-Band Frequency Range", *Health Scope*, vol. 5(3), pp. e30203, 2016.

[30] A. Andrea, A. Suarez, J. Torres, P. A. Martinez, R. Herraiz, A. Alcarria, A. Benedito, R. Ruiz, P. Galvez, and A. Penades, "Shielding Effectiveness Measurement Method for Planar Nanomaterial Samples Based on CNT Materials up to 18 GHz", *Magnetochemistry*, vol. 9, pp. 114, 2023.

[31] IEEE Standards Association, IEEE Std 2715-2023, "IEEE Guide for the Characterization of the Shielding Effectiveness of Planar Materials", *IEEE Electromagnetic Compatibility Society* Approved 15 February 2023.

[32] IEEE Standards Association, IEEE Std 521-2019, "IEEE Standard Letter Designations for Radar-Frequency Bands", *IEEE Aerospace and Electronic Systems Society*, Approved 7 November 2019.

[33] J. Baker-Jarvis, "Transmission/Reflection and Short-Circuit Line Permittivity Measurements", NIST Technical Note 1341, published by the National Institute of Standards and Technology (NIST), Boulder, CO, USA, 1990.

[34] B. Clarke, A. Gregory, D. Cannel, M. Patrick, S. Wylie, I. Youngs, and H. Hill, "A Guide to Characterization of Dielectric Materials at RF and Microwave Frequencies", London: NPL, 2003. ISBN:0904457389.

[35] C. Fan, B. Wu, R. Song, Y. Zhao, Y. Zhang, and D. He, "Electromagnetic shielding and multi-beam radiation with high conductivity multilayer graphene film", *Carbon*, vol. 155, pp. 506-513, 2019.

[36] A. Kaushal and V. Singh, "Electromagnetic interference shielding response of multiwall carbon nanotube/polypropylene nanocomposites prepared via melt processing technique", *Polymer Composites*, vol. 42, pp. 1148–1154, 2021.

[37] H. Oraby, I. Naeem, M. Darwish, M. H. Senna, and H. R. Tantawy, "Effective electromagnetic interference shielding using foamy polyurethane composites", *Polymer Composites*, vol. 42, pp. 3077, 2021.

[38] V. Shukla, "Review of electromagnetic interference shielding materials fabricated by iron ingredients", *Nanoscale Adv*, vol. 1, pp. 1640-1671, 2019.

[39] R. Kumar, S. R. Dhakate, T. Gupta, P. Saini, B. P. Singh, and R. M. Mathur, "Effective improvement of the properties of light weight carbon foam by decoration with multi-wall carbon nanotubes", *Journal of Materials Chem A*, vol. 1, pp. 5727-5735, 2013.

[40] R. Pal, S. L. Goyal, I. Rawal, and A. K. Gupta, "Tailoring of EMI shielding properties of polyaniline with MWCNTs embedment in X-band (8.2–12.4 GHz)", *Journal of Physics and Chemistry Solids*, vol. 169, pp. 110867, 2022.

[41] C. Liang, M. Hamidinejad, L. Ma, Z. Wang, and C. B. Park, "Lightweight and flexible graphene/SiC-nanowires/ poly(vinylidene fluoride) composites for electromagnetic interference shielding and thermal management", *Carbon*, vol. 156, no. 58-66, 2020.

[42] Z. Zeng, M. Chen, H. Jin, W. Li, X. Xue, L. Zhou, Y. Pei, H. Zhang, Z. Zhang, "Thin and flexible multi-walled carbon nanotube waterborne polyurethane composites with high-performance electromagnetic interference shielding", *Carbon*, vol. 96, pp. 768, 2016.

[43] K. Jagatheesan, A. Ramasamy, A. Das, and A. Basu, "Electromagnetic shielding behaviour of conductive filler composites and conductive fabrics – A review", *Indian Journal of Fibre & Textile Research*, vol. 39, pp. 329-342, 2014.

[44] H. Lv, X. Liang, G. Ji, H. Zhang, and Y. Du, "Porous three-dimensional flower-like Co/ CoO and its excellent electromagnetic absorption properties", *ACS Applied Material Interfaces*, vol. 7, pp. 9776–9783, 2015.

[45] C. Wang, Y. Ding, Y. Yuan, X. He, S. Wu, S. Hu, M. Zou, W. Zhao, L. Yang, A. Cao, and Y. Li, "Graphene aerogel composites derived from recycled cigarette filters for electromagnetic wave absorption", *Journal of Materials and Chemistry. C*, vol. 3, pp. 11893–11901, 2015.

[46] B. P. Singh, Prasanta, V. Choudhary, P. Saini, S. Pande, V. Singh, and R. Mathur, "Enhanced microwave shielding and mechanical properties of high loading MWCNT–epoxy composites", *Journal of Nanoparticle Research*, vol. 15, pp. 1, 2013.

[47] D. Bigg, "The effect of chemical exposure on the EMI shielding of conductive Plastics", *Polymer Composites*, vol. 8, no. 1, pp. 1–7, 1987.

[48] T. Peng, S. Wang, Z. Xu, T. Tang, and Y. Zhao, "Multifunctional MXene/Aramid Nanofiber Composite Films for Efficient Electromagnetic Interference Shielding and Repeatable Early Fire Detection", *ACS Omega*, vol. 7, no. 33, pp. 29161-29170, 2022.

[49] J. He, M. Han, K. Wen, C. Liu, W. Zhang, Y. Liu, X. Su, C. Zhang, and C. Liang, "Absorption-dominated electromagnetic interference shielding assembled composites based on modular design with infrared camouflage and response switching", *Composites Science and Technology*, vol. 231, pp. 109799, 2023.

[50] X. Hong, T. Peng, C. Zhu, J. Wan, and Y. Li, "Electromagnetic shielding, resistance temperature-sensitive behavior, and decoupling of interfacial electricity for reduced graphene oxide paper", *Journal of Alloys and Compounds*, vol. 882, pp. 160756, 2021.